Earth and Planetary Science Letters 444 (2016) 45–55

Contents lists available at ScienceDirect

Earth and Planetary Science Letters

www.elsevier.com/locate/epsl

Physical properties of volcanic lightning: Constraints from magnetotelluric and video observations at Sakurajima volcano, Japan

Koki Aizawa [a,*], Corrado Cimarelli [b], Miguel A. Alatorre-Ibargüengoitia [c], Akihiko Yokoo [d], Donald B. Dingwell [b], Masato Iguchi [e]

[a] Institute of Seismology and Volcanology, Faculty of Sciences, Kyushu University, 2-5643-29 Shin'yama, Shimabara, Nagasaki 855-0843, Japan
[b] Department of Earth and Environmental Sciences, Ludwig Maximilian University of Munich, Theresienstraße 41, 80333 Munich, Germany
[c] Centro de Investigación en Gestión de Riesgos y Cambio Climático, Universidad de Ciencias y Artes de Chiapas, Tuxtla Gutiérrez, Chiapas 29039, Mexico
[d] Aso Volcanological Laboratory, Institute for Geothermal Sciences, Graduate School of Science, Kyoto University, Japan
[e] Sakurajima Volcano Research Center, Disaster Prevention Research Institute, Kyoto University, Yokoyama 1722-19, Sakurajima, Kagoshima 891-1419, Japan

A R T I C L E   I N F O

Article history:
Received 31 October 2015
Received in revised form 8 March 2016
Accepted 11 March 2016
Available online 5 April 2016
Editor: T.A. Mather

Keywords:
volcanic lightning
magnetotelluric
high speed video
Sakurajima
volcanic plume
thunderstorm lightning

A B S T R A C T

The lightning generated by explosive volcanic eruptions is of interest not only as a promising technique for monitoring volcanic activity, but also for its broader implications and possible role in the origin of life on Earth, and its impact on the atmosphere and biosphere of the planet. However, at present the genetic mechanisms and physical properties of volcanic lightning remain poorly understood, as compared to our understanding of thundercloud lightning. Here, we present joint magnetotelluric (MT) data and video imagery that were used to investigate the physical properties of electrical discharges generated during explosive activity at Sakurajima volcano, Japan, and we compare these data with the characteristics of thundercloud lightning. Using two weeks of high-sensitivity, high-sample-rate MT data recorded in 2013, we detected weak electromagnetic signals radiated by volcanic lightning close to the crater. By carefully inspecting all MT waveforms that synchronized with visible flashes, and comparing with high-speed (3000 frame/s) and normal-speed (30 frame/s) videos, we identified two types of discharges. The first type consists of impulses (Type A) and is interpreted as cloud-to-ground (CG) lightning. The second type is characterized by weak electromagnetic variations with multiple peaks (Type B), and is interpreted as intra-cloud (IC) lightning. In addition, we observed a hybrid MT event wherein a continuous weak current accompanied Type A discharge. The observed features of volcanic lightning are similar to thunderstorm lightning, and the physical characteristics show that volcanic lightning can be treated as a miniature version of thunderstorm lightning in many respects. The overall duration, length, inter-stroke interval, peak current, and charge transfer all exhibit values 1–2 orders of magnitude smaller than those of thunderstorm lightning, thus suggesting a scaling relation between volcanic and thunderstorm lightning parameters that is independent of the type of charged particles. On the other hand, the polarities, which are estimated by long-time (3.4 yrs) MT (32 samples/s) and video (30 frame/s) observations, are different than those of normal thunderstorm lightning. These observations are consistent with the notion that charge structures in volcanic ash plumes are highly disordered and are characterized by numerous small charged regions with high charge density.

1. Introduction

Explosive volcanic eruptions frequently generate lightning within and around the eruptive plume. Volcanic lightning is a consequence of plume electrification. Possible mechanisms for plume electrification include fractoemission, particle–particle collisions, boiling of water and the presence of ice and ice-coated particles in the eruptive column (e.g., Buttner et al., 2000; James et al., 2000; Mather and Harrison, 2006; Thomas et al., 2007; James et al., 2008), all of which may result in volcanic lightning by the separation of electrically charged particles. Since a scientific report on the 1963 eruption of Surtsey volcano, Iceland (Anderson et al., 1965), volcanic lightning has been documented intermittently (Brook et al., 1974; Mather and Harrison, 2006; James et al., 2008; McNutt and Williams, 2010). Volcanic lightning

* Corresponding author. Tel.: +81 957 62 6621; fax: +81 957 63 0225.
E-mail addresses: aizawa@sevo.kyushu-u.ac.jp (K. Aizawa), cimarelli@min.uni-muenchen.de (C. Cimarelli), miguel.alatorre@unicach.mx (M.A. Alatorre-Ibargüengoitia), yokoo@aso.vgs.kyoto-u.ac.jp (A. Yokoo), dingwell@lmu.de (D.B. Dingwell), Iguchi@svo.dpri.kyoto-u.ac.jp (M. Iguchi).

http://dx.doi.org/10.1016/j.epsl.2016.03.024
0012-821X/

has been used to monitor volcanic plumes even under adverse weather conditions (McNutt and Davis, 2000; Behnke and McNutt, 2014), and also to investigate inner plume dynamics (Behnke and Bruning, 2015). Particle electrification and discharge (lightning) influence the aggregation of ash particles and ash transport dynamics (Carey and Sigurdsson, 1982; Mather and Harrison, 2006; James et al., 2008). Furthermore, volcanic lightning may impact the Earth's environment (and that of other planets) by fixing nitrogen in a variety of chemical forms, as NO, NO_2, HNO_3, and NH_3 (Mather et al., 2004a). Such NO_x species have a significant impact on ozone concentrations in the atmosphere, and on the fundamental conditions required for the origin and early evolution of life on Earth (Navarro-Gonzalez et al., 1998). However, advancements in our understanding of volcanic lightning, and their impact on the atmosphere and biosphere, have been hampered by our limited understanding of the genetic mechanisms and physical parameters of volcanic lightning.

To understand the physical mechanism of volcanic lightning, one useful approach is to compare and contrast with thunderstorm lightning, which has been studied in increasing detail for decades (e.g., Rakov and Uman, 2003). Based on studies of thunderstorm lightning, particularly the well-studied cloud-to-ground (CG) type, the physical cycle of a lightning discharge can be summarized as follows: (1) collisions of hydrometeors result in electrification; (2) the electric field intensifies due to particle (and hence charge) separation; (3) dielectric breakdown of air results in the development of a conducting channel of ionized gas (a column of charge), called a stepped leader, which propagates in a stepped manner; and (4) rapid transfer of electric charge, the so-called return stroke, which is accompanied by bright optical flashes. Processes (3) and (4) can occur more than once in a single lightning event. In the case of a partially conducting condition of the return stroke channel, a dart leader can be generated, which propagates more rapidly than the stepped leader. A return stroke is often followed by a relatively weak continuing current that persists for tens to hundreds of milliseconds. To date, there has been a lack of observational evidence enabling comparisons of the processes of volcanic and thundercloud lightning.

In the past 10 yrs, modern lightning detection techniques, based on electromagnetic (EM) field radiation in the very high frequency (VHF) range (30 MHz–0.3 GHz), have been used to study Augustine, Redoubt, and Eyjafjallajökull volcanoes (Thomas et al., 2007; Behnke et al., 2013, 2014). Using a VHF array network and the time-of-arrival technique, VHF sources can be located with high precision. Because VHF radiation is generated by dielectric breakdown (e.g., Rakov and Uman, 2003; Behnke and McNutt, 2014), the development of the lightning channel is estimated from the spatio-temporal evolution of VHF sources. Due to its high sensitivity, even a single VHF station is useful in detecting the occurrence of lightning; thus, VHF measurement is a powerful technique in studies of volcanic lightning in particular. However, VHF radiation significantly weakens when the source is not within line-of-sight of the observation point, and VHF sources are essentially not radiated when very strong current flows are associated with process (4). Therefore, in order to capture the complete lightning cycle, it is also necessary to observe the electromagnetic (EM) field at lower frequencies.

Array networks capable of observing radio pulses in the very low frequency range (VLF: 3–30 kHz) have been widely used to monitor thunderstorm lightning. Because VLF signals travel long distances in the waveguide formed between Earth's surface and the ionosphere, these systems cover wide areas and can occasionally be used to detect electrical activity associated with volcanic eruptions. For example, ATDnet, which operates in the UK in a narrow frequency band (~10–14 kHz), detected volcanic lightning during the 2010 Eyjafjallajökull eruption in Iceland (Bennett et al., 2010; Arason et al., 2011). Compared with VHF observations, VLF observations have the advantage of detecting return strokes associated with CG lightning. However, the station coverage in a VLF network is typically too sparse for long-range detection. Weak EM radiation events, originating close to the active vent, are therefore rarely detected (Bennett et al., 2010). Furthermore, when the source and observation sites are several hundreds of kilometers apart, VLF waveforms are strongly influenced by the properties of the propagation path (e.g., Rakov and Uman, 2003). Although a VLF lightning detection network is useful for detecting large eruptions, a custom-designed observation system is needed to study all of the physical processes involved in volcanic lightning. Such regional VLF networks have been deployed to study thunderstorm lightning in Florida, USA (Shao et al., 2006), Alabama, USA (Bitzer et al., 2013), and Europe (Betz et al., 2009), but such a network has not been previously deployed around an active volcano.

Magnetotellurics (MT) is a method commonly used to image subsurface electrical resistivity structure (e.g., Simpson and Bahr, 2005) and its temporal changes (e.g., Aizawa et al., 2011). The MT method, which usually measures two horizontal electric field components and three magnetic field components at the Earth's surface, has recently been used to study volcanic lightning at Sakurajima volcano, Japan (Aizawa et al., 2010). Although the time resolution depends on the sampling rate, MT covers broad-band EM signals with a high dynamic range (24 bit A/D conversion), and therefore can detect weak signals whose amplitudes are smaller than military VLF noise. As compared with conventional antennas used in thunderstorm lightning research, the unique and valuable aspect of MT is that it reproduces true waveforms in real physical units; this is because the frequency characteristics of the sensors and the data logger are all accurately determined in the laboratory. With the MT method, it is possible to determine the timing and polarity of lightning by measuring electromagnetic field variations caused by volcanic lightning, even at distances of several kilometers. However, due to the low sampling rate (as low as 15 samples per second (sps)), the previous study (Aizawa et al., 2010) could not investigate the physical properties of the volcanic lightning cycle; e.g., waveform, electric current, and duration.

In this study, we present new MT data recorded at higher sampling rates (32 sps and 65,536 sps), which are visually correlated with normal and high-speed video observations (at 30 and 3000 frames per second (fps), respectively) in order to study the properties of vent discharges and near-vent lightning (Thomas et al., 2012; Behnke et al., 2013) at Sakurajima volcano, Japan. The high-speed (HS) camera is a powerful tool for investigating the spatio-temporal characteristics of lightning development, and it has recently been applied to thunderstorm lightning research (e.g., Mazur et al., 1995; Ballarotti et al., 2005). Recent HS video observations of volcanic lightning at Sakurajima volcano (Cimarelli et al., in press) confirm the presence of stepped leaders and return strokes. However, the time scale of return strokes, return stroke multiplicity, the existence of continuing current, and the electromagnetic parameters that characterize volcanic lightning have yet to be investigated. Here, we provide observational evidence that allows a comparison of the processes of volcanic and thunderstorm lightning, and we derive estimates of the physical properties of volcanic lightning, especially electromagnetic field variations. In addition, we report on the polarities of volcanic lightning and the inclinations of lightning paths relative to wind directions, examined over a period of 3.4 yrs, using both MT (32 sps) and video (30 fps) observations.

2. Observations

Sakurajima volcano is one of the most active volcanoes in Japan. After June 2006, volcanic activity shifted from Minami-dake crater

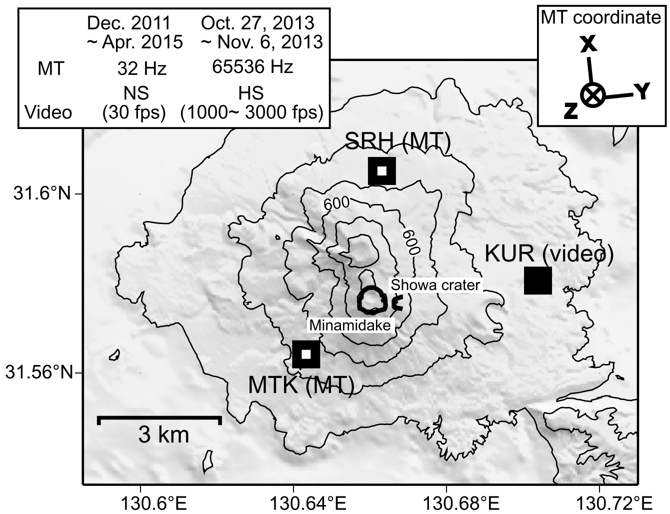

Fig. 1. Topographic map showing the locations of MT (open squares) and video stations (solid squares) at Sakurajima volcano, Japan. Eruptive vents are indicated by thick solid lines. Contour interval is 200 m.

(at the summit) to the persistently active Showa crater, 500 m east of the summit (Fig. 1). According to the Japan Meteorological Agency (JMA), 1097 eruptions occurred at Showa crater in 2013, while no eruptions were recorded in 2013 at Minami-dake crater. Videos of volcanic lightning were recorded from the Kurokami observatory of Kyoto University (KUR), located 3.5 km east of Showa crater, with a direct view of the Showa crater rim. MT data were recorded at two sites, approximately 2.2 and 3.5 km from Showa crater, respectively (Fig. 1).

The MT data and video recordings are divided into two datasets based on record duration and sampling rate. The first dataset was obtained between December 2011 and April 2015. In this period, MT data were continuously recorded at 32 sps by two Metronix ADU07 systems, which record five GPS-synchronized electromagnetic time series (two horizontal electric fields, two horizontal magnetic fields, and a vertical magnetic field). Additionally, we developed a video recording system at KUR. Time-synchronized video was digitally captured and recorded continuously in HDD at normal speed (NS, 30 fps) using a high-sensitivity camera (Hitachi KP-DE500, Hitachi Kokusai Electric) and a PC. Time-stamped video frames were obtained using a time code generator with a GPS clock, as in the work of Yokoo et al. (2009).

The second dataset was obtained between late October and early November 2013. During October 26, November 5, and November 10–12, MT data were recorded at 65 ksps (65,536 sps) using induction coils (MFS07 and MFS07e) whose frequency responses were calibrated to 60 kHz in the laboratory. During this period, time-synchronized videos were recorded at frame rates of 1000 and 3000 fps by two high-speed (HS) cameras (Vision Research Phantom v710 and v711) and an IRIG-B GPS time-signal generator. The time precision of the GPS time system is within 20 ns. The exposure time of the sensor is chosen in proportion to the sampling rate (0.333 ms in the case of a sampling rate of 3000 fps). HS video recordings were manually triggered by the occurrence of any visible flash associated with the ash plume (Cimarelli et al., in press). Continuous observations of electric activity in the plume were made possible by the NS (30 fps) camera. In addition, we recorded infrasound data at KUR to characterize the explosivity of the eruptions.

In this study, we processed raw 24-bit MT time series data by applying a Fourier transform and incorporating the frequency responses of the logger and induction coils. Time series (in physical units of V/m and nT) were then obtained by an inverse Fourier transform. DC and low-frequency variations were removed by applying a high pass filter which cuts the signal in the frequencies lower than 0.3 Hz. Therefore, using 65-ksps observations, we reproduced the true EM waveform in the frequency range of 32 kHz–0.3 Hz, which covers VLF (3–30 kHz), ULF (0.3–3 kHz), SLF (30–300 Hz), and ELF (3–30 Hz) ranges. In addition, we eliminated VLF military noise in the 65 ksps time series by applying a digital notch filter (Fig. 2). Notch filtering is essential for delineating weak EM radiation.

3. Physical properties of volcanic lightning

3.1. Constraints from high-rate data sampling

During the 2013 campaign, simultaneous MT and video data (NS and HS) were successfully recorded for nine eruptions. Two additional eruptions on November 11 were only recorded at site MTK and by NS video (Table 1). We carefully examined the MT time series corresponding to times when the NS videos showed visible flashes, and observed MT signals above background noise levels for 100 of 111 (90.1%) recorded optical flashes. Note that the HS-camera captured more optical flashes than the NS-camera (Cimarelli et al., in press). After careful inspection of all MT waveforms coinciding with visible NS video flashes, we recognized two types of discharge events, herein referred to as Type A and Type B. A waveform for a Type A event consists of 1–9 unipolar impulses, each having durations on the order of a few tens of µs. In these events with multiple impulses, the duration from the first to the last impulse is approximately 1–8 ms (Figs. 2b and 3). Type B exhibits multiple peaks and the repose between each peak is indistinct (Fig. 2c). The total duration of Type B discharges is approximately 0.5–4 ms, and the magnetic field components usually favor one polarity. The durations of Type B discharges are much longer than each impulse in Type A waveforms, but they are usually shorter than the total duration of a Type A event (Figs. 2 and 3).

Fig. 4 shows an example of HS video and corresponding MT time series data for a Type A discharge. A small optical emission and dark dielectric breakdown signature are seen in frame 2 of the video, which corresponds to the onset of EM radiation. A unipolar impulse first occurs when a bright emission is recorded in the video (frame 3). Another pulse is recorded in concomitance with a much brighter emission (frame 7). These two frames of the video show a possible connection between the lightning channel and the ground at different points. Based on the correspondence between the optical lightning shape and the MT waveform, we infer that Type A events can be categorized as CG. Very bright optical flashes in NS videos always coincide with Type A signals, supporting this hypothesis. CG lightning in thunderstorms is similar to Type A, in that it shows single or multiple strong impulses that correspond to return strokes. However, it should be noted that thunderstorm lightning also shows weak impulses from other charge-moving processes in a cloud (e.g., Rakov and Uman, 2003). Given the limited statistics presented in this study, we cannot a priori discard the possibility that Type A waveforms can also be produced by IC discharges in volcanic lightning.

From the polarities of magnetic field variations, and assuming that the electric current flows vertically, we determined the polarity of Type A discharges observed during the 2013 campaign. A total of 31 of 42 (74%) Type A discharges were lightning transferring negative charge to the ground. Both positive and negative polarities were observed during a single eruption. Note that the impulses in Figs. 2–4 are all interpreted as −CG lightning, which lowers negative charge to the ground.

The durations of Type A lightning (1–8 ms) are short relative to CG lightning in thunderstorms, which lasts for tens to hundreds

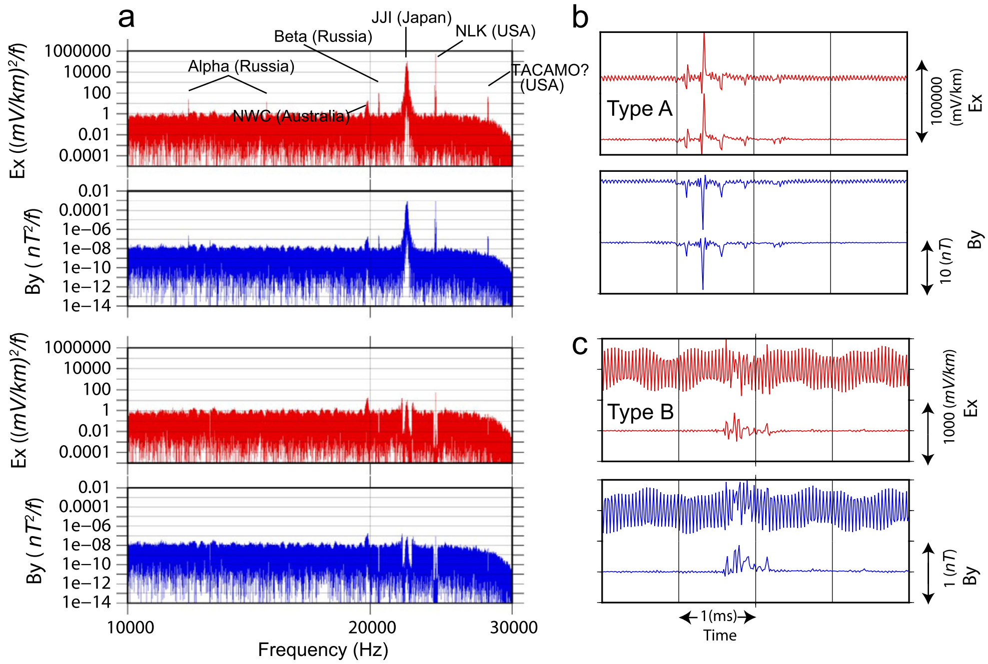

Fig. 2. Notch filtering applied to 65 kHz sampled MT data for eliminating military VLF noise. (a) Raw and notched spectra of the N–S electric field (Ex) and E–W geomagnetic field (By) at site SRH. Horizontal axis has a logarithmic scale. Following the usual MT convention, the north (x), east (y), and downward (z) fields are assigned positive values. The codes noted above each peak show military signals for submarine communications. (b) MT data showing an example of volcanic lightning at 21:31:59.2 JST, 30 October 2013. The upper and lower panels are raw and notch filtered waveforms, respectively. The waveform consists of five impulses. We refer to such waveforms as Type A discharges in the text. (c) MT data showing an example of volcanic lightning at 21:32:17.3 JST on 30 October 2013. The waveform is like an EM variations with multiple peaks that continues for ∼1 ms; we refer to such waveforms as Type B discharges in the text.

Table 1
Studied eruptions and occurrences of volcanic lightning.

Eruption start time (JST/UTC + 9)	Plume height (m above crater)	Maximum amplitude of infrasound record at Kurokami (Pa)	Number of flashes seen in NS (30 fps) video	Type of MT waveform		
				Type A (and total pulses)	Type B	Signal undetectable
10/27/2013 19:32	1600	121	6	2 (3)	3	1
10/27/2013 20:56	2000	212	6	1 (3)	4	1
10/27/2013 22:04	2200	418	12	0	8	4
10/30/2013 0:02	1400	31	3	1 (1)	2	0
10/30/2013 1:36	1800	52	2	1 (1)	1	0
10/30/2013 20:45	1800	59	4	1 (1)	3	0
10/30/2013 21:30	2400	128	22	15 (39)	6	1
11/11/2013 19:46[a]	1600	<1	8	1 (9)	5	2
11/11/2013 19:48[a]	1800	<1	48	20 (61)	26	2

Notes: Visible flashes observed in 30 fps movies and corresponding EM discharge types in 65 kHz sampling MT data. In Type A column, the number of flashes and total number of pulses are shown, respectively. Some flashes are not accompanied by a significant MT signal (i.e., not above background noise levels). Data of plume height is obtained by JMA.
[a] Eruptions for which MT data are only available from station MTK.

of ms (Berger et al., 1975; Rakov and Uman, 2003; Ballarotti et al., 2012). Although afterglow persists for up to 200 ms in NS videos and 26 ms in HS videos (Cimarelli et al., in press), a corresponding MT signal was not detected. This afterglow may represent high-temperature regions in the lightning path, and its brightness and duration in the recordings may depend strongly on camera sensitivity. We therefore do not discuss afterglow duration further here.

Assuming a magneto-static approximation associated with a vertical electric current (Rakov and Uman, 2003), the relationship between observed magnetic field (T) and electric current (a current dipole) along the lightning path can be expressed as

$$B(r) = \frac{\mu_0}{2\pi r}\left[\frac{H_m}{R(H_m)}\right]I, \tag{1}$$

where I is the current of the CG lightning, r is the distance between the point struck by lightning and the observation site, H_m is the vertical length of the lightning, and $R(H_m)$ is the distance between the lighting top and the observation site. A Type A discharge, interpreted as CG, is visible at 21:32:55.7 Japan Standard Time (JST) on 2013-10-30 in the 30 fps video (Fig. 3). The apparent vertical length is ∼300 m. This event is very bright, but not unusual among NS video recordings between December 2011 and April 2015. At station SRH, the amplitudes of B field pulses in the 65 kHz sampling records are approximately $20 \cdot 10^{-9}$ T. Letting $r = R(H_m) = 3500$ m, and $H_m = 300$ m, the observed $B(r)$ from the MT yields an estimated $I = 2$ kA. Repeating this calculation for the event of Fig. 4 (with $H_m = 100$ m, $B = 5 \cdot 10^{-9}$ T) yields $I \sim 1$ kA, which is smaller by 1–2 orders of magnitude than typical values for −CG return strokes in thunderstorms (Berger et al., 1975; Rakov and Uman, 2003; Visacro et al., 2004). From Fig. 3c, the calculated charge transfer of the return stroke is ∼0.05 C, which is also smaller by two orders of magnitude than typical thunderstorm values (Berger et al., 1975; Rakov and Uman, 2003; Visacro et al., 2004).

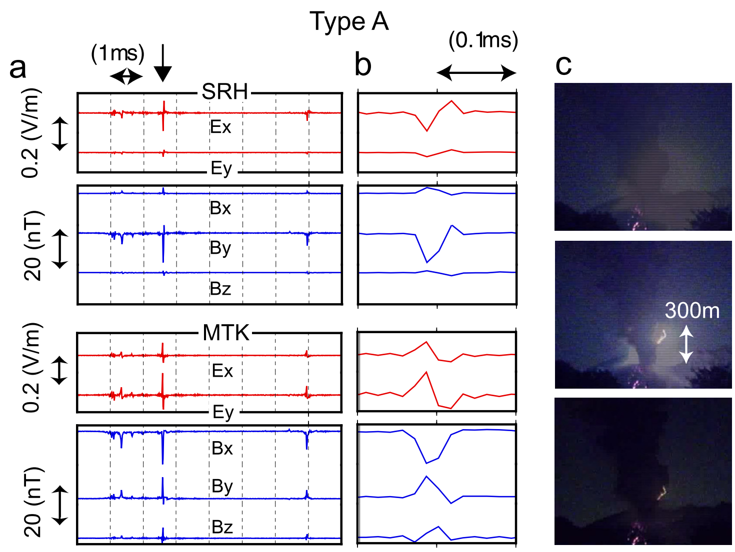

Fig. 3. Type A MT waveform associated with volcanic lightning at 21:32:55.7 JST on 30 October 2013. (a) The 65 kHz MT data recorded at stations SRH and MTK (Fig. 1). (b) Close-up of the pulse indicated by the vertical arrow in (a). The signal arrived at both MT sites simultaneously, to within the limit of time resolution. (c) Consecutive frames from the NS (30 fps) video for the event in (a). The frame interval is 33.3 ms. Note that corresponding HS video does not exist for this event.

Fig. 5 shows an example of MT time series and high-speed images of two Type B discharges. The two EM variations with multiple peaks (Type B discharges) correspond to relatively bright optical emissions. As the terminations of the lightning paths do not touch the ground (as observed in the HS videos), we interpret Type B events as IC. All NS videos from the 2013 campaign show no Type B discharges corresponding to CG lightning. The waveforms of Type B may be similar to those of IC lightning in thunderstorms (e.g., Kitagawa and Brook, 1960; Zhu et al., 2014). From MT data, the total durations of Type B discharges are ∼0.5–4 ms, which is, again, two orders of magnitude smaller than typical values for IC lightning in thunderstorms (Rakov and Uman, 2003).

In addition to isolated Type A and B events, a rare third type of waveform (showing continuing change) was found. Fig. 6 shows MT data recorded at 19:49:8.7 JST on 11 November 2013, 58 s after the onset of the eruption. Both Type B and Type A discharges were observed in a time lapse of 20 ms. From the NS video, we interpret Type B as IC and Type A as CG. A rare feature of this sequence is a slow change in the magnetic field that lasts ∼5 ms after the Type A discharge. Because magnetic field variations are primarily related to the electric current in the lightning path, this observation indicates the presence of a weak continuing current. In thunderstorm lightning studies, a continuing current (CC) is defined as a relatively small current that persists after the return stroke, and its duration can be classified as "long" ($t > 40$ ms), "short" ($10 \text{ ms} < t \leq 40$ ms), or "very short" ($3 \text{ ms} < t < 10$ ms) (Ballarotti et al., 2005). One notable feature of the CC is a large electric charge transfer, comparable to those of return strokes. From the magnetic field change in Fig. 6, using equation (1) with $R(H_m) = 2200$ m and $H_m = 300$ m, the average electric current is calculated as ∼20 A. Charge transfer is thus $20 \text{ A} \cdot 5 \text{ ms} = 0.1$ C, comparable to the return strokes in Figs. 3–4. Thus, volcanic lightning is also similar to thunderstorm lighting in that it presents an accompanying CC, but its electric current and charge transfer are 1–2 orders of magnitude smaller than those of thunderstorm lightning (Fisher et al., 1993; Rakov and Uman, 2003). In addition, there may be a difference in the timing of occurrence of the CC. In Fig. 6, CC begins 0.3 ms before the Type A impulse (i.e. the return stroke). On the other hand, CC waveforms in thunderstorm lightning have been observed following the first return stroke (Fisher et al., 1993).

3.2. Constraints from low-rate data sampling

We also analyzed 32 Hz MT data from eruptive events recorded between December 2011 and April 2015. During this time, MT data from 588 eruptions were recorded at both MT stations, along with NS video of the active crater. Due to the low sampling rate (32 Hz), Types A and B cannot be distinguished because all signals are recorded as pulses. These were previously referred to as "MT pulses" by Aizawa et al. (2010). In this study, we used MT data from 5 min before to 10 min after the eruption onset (defined as the time when the ash plume emerged from the crater rim, as observed in the videos), and defined MT pulses as cases where amplitudes of horizontal electric and horizontal geomagnetic fields at both observation sites simultaneously exceeded 0.003 mV/m and 0.03 nT, which are approximately ten times higher than the background EM variations in the 32-sps time series. By using amplitude ratios of B_x and B_y at each site, we used magnetic field direction finding to estimate the source locations of EM radiators. This is essential to discriminate volcanic lightning from distant thunderstorm lightning or artificial noise. We did not use electric fields in this step, because they possibly include a substantial induction effect (e.g., Simpson and Bahr, 2005; Chave and Jones, 2012); thus, we believe that the electric field cannot be explained solely by voltage differences resulting from direct electric current injection into the earth (Kitagawa, 2005). Rather, the field is also influenced by EM induction. Fig. 7a shows the estimated source locations. Since volcanic lightning paths are not always vertical, the estimated source locations are scattered around the crater. According to the theory of magnetic direction findings (Uman et al., 1980), the error of the estimated direction increases as the lightning path is increasingly oblique to the vertical axis and trends parallel to a line from the crater to the observation site. On the other hand, the direction error is negligible when the lightning path is oblique to the vertical axis and trends perpendicular to a line from the crater to the observation site. At Sakurajima, the ENE–WSW-trending distribution is due to a relatively poor source direction determined from station SRH, which is explained by assuming that lightning paths tend to be inclined to station SRH (i.e., the N–S direction). It should be noted here that the N–S direction is approximately consistent with the prevalent wind direction (NNW–SSE) around Sakurajima volcano. From the estimated EM radiators (Fig. 7a), it is apparent that the lightning paths tend

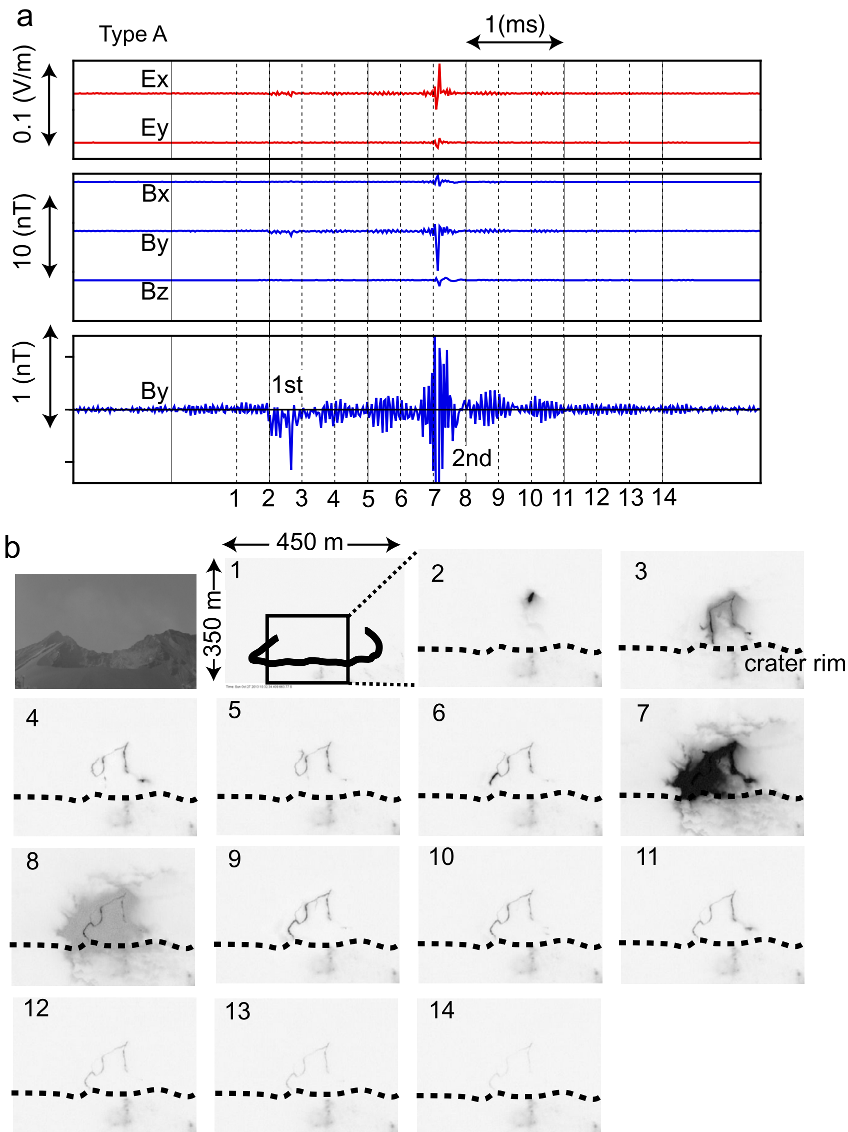

Fig. 4. MT time series and corresponding HS-video (3000 fps) beginning at 19:32:34.4 JST on 27 October 2013. (a) MT data at site SRH. The discharge is classified as Type A, and includes two pulses. Numbers (1–14) correspond to frame numbers shown in (b). (b) Time-lapse pictures taken from HS-video. The time interval between each frame is 0.333 ms. The Showa crater rim is indicated in frame 1 by a solid line. Frames 2–14 are close-ups of frame 1. Black strings correspond to the bright part of the lightning path. Brighter strokes that possibly connect from cloud to ground are found in frames 3 and 7. The locations struck by lightning in frames 3 and 7 are different in each case.

to be inclined relative to the vertical axis, toward the dominant wind direction around Sakurajima, which in turn coincides with the prevalent dispersal direction of volcanic ash. In this study, we assumed that all EM radiator locations within 2.0 km of Showa crater were caused by volcanic lighting. Thunderstorm lightning within a 2-km radius of the crater is considered to be negligible, mainly because we used MT data when the crater was visible from the KUR site; i.e., under clement weather conditions. The presence of artificial noise within 2 km of the crater is also unlikely, as no electric facilities exist in this area. Employing this criterion, 533 total MT pulses were identified in 163 of the 588 eruptions recorded. When identified on NS video, these pulses corresponded to bright, possibly CG lightning. Fig. 7b shows the temporal distribution of pulses relative to time since eruption onset. Both positive and negative MT pulses occurred at Sakurajima volcano, making up 34.3% and 65.6% of the total pulses, respectively. This polarity distribution differs from that of usual thunderstorm lightning, in which negative CG lightning is typically dominant (Rakov and Uman, 2003).

4. Discussion

Before making further comparisons with thunderstorm lightning, we note here that our observations correspond only to specific types of volcanic lightning. According to the classification proposed by Thomas et al. (2012), based on observations of Augustine volcano, the volcanic lightning events reported here are most likely “vent discharges” or “near-vent discharges” that occur during volcanic plume growth. “Plume lightning” events (i.e., lightning that forms inside and around large plumes) were not observed in this study. Plume lightning is possibly caused by the charging of colliding ash nuclei coated with ice (Thomas et al., 2007, 2012), but ice formation is unlikely in the erupted plume of the studied eruptions (Cimarelli et al., in press). It should also be noted that “very small flashes (sparks)” of centimeter to meter length, as generated in particle-laden jet experiments by Cimarelli et al. (2014), may well be generated at Sakurajima. However, these fall below the limit of detection of our systems, and therefore they cannot be accounted for in this study. Indeed, 9.9% of visible flashes in NS videos, which

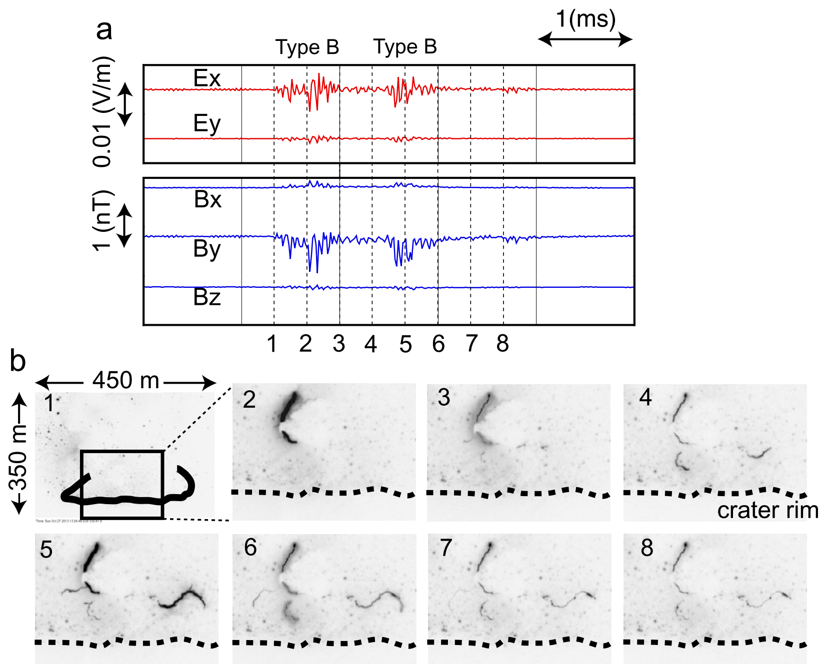

Fig. 5. MT time series and corresponding HS-movie beginning at 22:04:09.2 JST on 27 October 2013. (a) MT data at site SRH. The discharge is Type B, in which two EM variations are found. The durations of Type B discharges are much longer than each pulse in Type A waveforms. (b) Still frames taken from HS-movie. The black dots are volcanic ejecta. Two relatively bright IC flashes are found in frames 2 and 5.

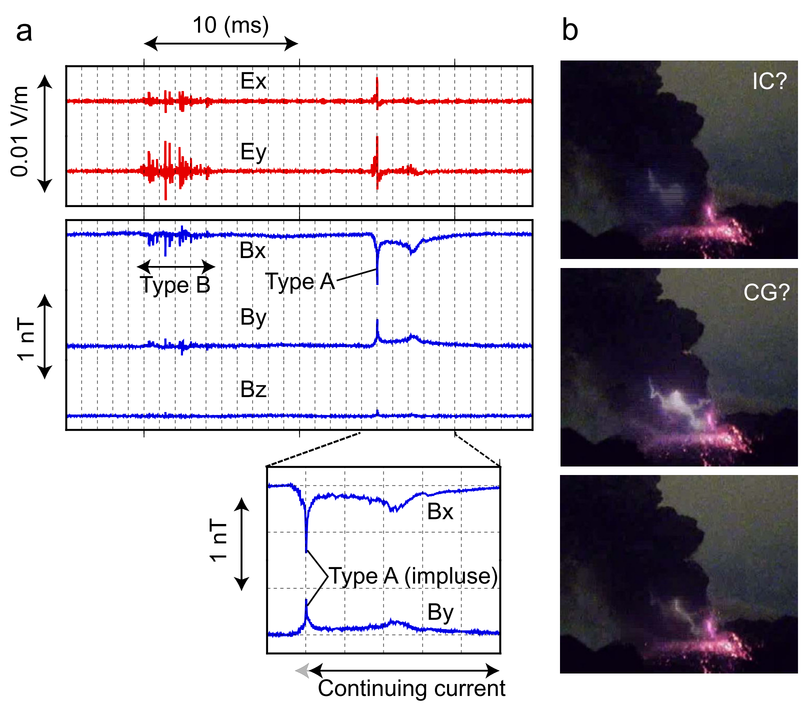

Fig. 6. MT time series and corresponding NS video, beginning at 19:49:8.7 JST on 11 November 2013. (a) MT data at site MTK. Discharges are labeled with their interpreted types. Lower panel shows a close-up of magnetic field recordings, in which a continuing current lasts for ~5 ms. (b) Consecutive frames from 30 fps video, showing the events of panel (a). The frame interval is 33.3 ms.

are relatively small and less bright, had no detectable MT signature (Table 1).

Volcanic lightning at Sakurajima is similar to thunderstorm lightning in that it shows leaders, multiple return strokes, and continuing current. Comparative physical properties of negative CG thunderstorm lightning and volcanic lightning at Sakurajima are summarized in Table 2. The parameter ranges for volcanic lightning were determined from all data in our possession, including detailed analyses of high-speed videos (Cimarelli et al., in press). The parameters of thunderstorm lightning were taken from previous studies (Berger et al., 1975; Rakov and Uman, 2003; Visacro et al., 2004; Ballarotti et al., 2012, and references therein). In this study, we do not discuss the physical properties of IC type lightning, due to complicating factors that include (1) complex lightning path, (2) complex waveforms, and (3) weak signals.

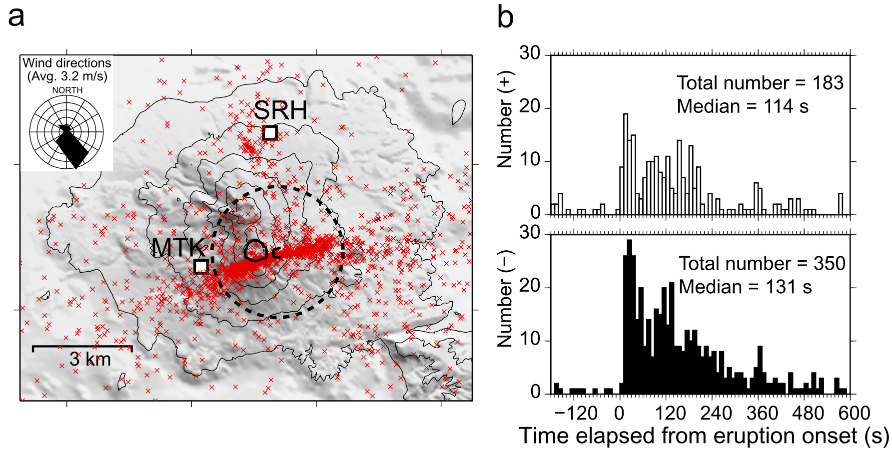

Fig. 7. Locations of EM radiators and histograms of EM pulses, possibly from CG volcanic lightning, December 2011 to April 2015. (a) Locations of EM radiators (red cross symbols) estimated by magnetic field direction finding. EM radiators within the dashed circle (2 km radius) are interpreted as volcanic lightning. The inset rose diagram shows the dominant wind directions (North to South) measured at the Japan Meteorological Agency branch office in Kagoshima city. (b) Histogram of MT pulses located within the circle in (a). Positive and negative MT pulses, interpreted as +CG and −CG lightning, are shown on the upper and lower plots, respectively. MT pulses before eruption onsets are possibly either from plumes emitted before the eruption onset, or from sources unrelated to volcanic lightning.

Table 2
Comparison of volcanic lightning and thunderstorm lightning.

	Parameter	Volcanic lightning at Sakurajima	Thunderstorm lightning
Overall	Duration	0.1–8 ms	200–300 ms
	Interstroke interval	1–5 ms	60 ms
	Number of return strokes per flash	1–9 (2.8 in 50%)[a]	1–18 (5.2 in 50%)
	Length	10–495 m[b]	7000 m
	Polarity	26% (34%) positive 74% (66%) negative	10% positive 90% negative
Dielectric breakdown	Speed (length/duration)	$1.2 \cdot 10^5$ m/s[b]	$2 \cdot 10^5$ m/s
Return stroke	Duration	30 μs (to the end)	70–80 μs (to half-peak value)
	Peak current	2 kA	30 kA (half-peak value)
	Charge transfer	0.05 C	5 C
Continuing current	Duration	5 ms	–200 ms
	Magnitude	20 A	–200 A
	Charge transfer	0.1 C	–20 C

Notes: Physical parameters of cloud-to-ground (CG) volcanic lightning at Sakurajima, and corresponding typical properties of CG thunderstorm lightning. Polarities in parentheses are estimated from December 2011 to April 2015. Other values are estimated from campaign observations in 2013.

[a] Number of return strokes per optical flash at Sakurajima, as estimated from the multiplicity of Type A discharges. Note: it is also possible that Type A waveforms can be produced by IC discharge.

[b] Data are from another paper (Cimarelli et al., in press). Typical parameters in thunderstorm lightning are taken from previous studies (Berger et al., 1975; Rakov and Uman, 2003; Visacro et al., 2004; Ballarotti et al., 2012, and references therein).

The data presented in Table 2 are consistent with the suggestion that the volcanic lightning recorded in this study is a miniature-scale equivalent of thunderstorm lightning in many respects. The overall duration, length, inter-stroke interval, peak current, and charge transfer are all 1–2 orders of magnitude smaller than corresponding values for thunderstorm lightning. The charge transfer of the continuing current is also 1–2 orders of magnitude smaller. On the other hand, the speeds of stepped leader (dielectric breakdown) are similar between the two types of lightning. These observations suggest that the differences between volcanic lightning and thunderstorm lightning are predominantly derived from differences in length and time scales. This result suggests the existence of a scaling law in these lightning parameters (e.g., small lightning transfers small charges over a short time scale) regardless of the type of charged particles. The scaling relation may be controlled by the electric charge densities in thunderclouds and volcanic plumes (McNutt and Williams, 2010). The maximum electric field (V/m) at the surface of a uniformly charged spherical volume of radius R is theoretically expressed as

$$E = \frac{\rho R}{3\varepsilon_0}, \quad (2)$$

where ρ is the space charge density (C/m^3) and ε_0 is the dielectric permittivity. The maximum field between two uniformly charged spherical volumes of opposite polarity is twice this value. Assuming that (1) the space charge density in a volcanic plume is higher than that in a thundercloud, and (2) the dielectric strength in the volcanic plume is similar to that in a thundercloud, then it follows that volcanic lightning occurs in cases of small R, which is consistent with observations. The short length and small charge transfer of volcanic lightning at Sakurajima can be explained by the existence of many small charged regions with strong charge density. If the scaling relation holds, then the volcanic lightning reproduced in the laboratory by Cimarelli et al. (2014) may have occurred at stronger charge density. Further observations are needed to confirm this hypothesis. In particular, measurements of the charge densities in thunderclouds, volcanic plumes, and ash-laden jet experiments would be required; these measures could then compared with electric charge transfers and lightning lengths.

Dissimilarity from the general behavior above consists in lightning polarities (Table 2). This discrepancy may be related to differences in electric charge structures between volcanic plumes and thunderstorm clouds, which is also indicated by the short length and small charge transfer of volcanic lighting at Sakurajima. We posit that the electric charges in a volcanic plume have a complex structure, with many pocket-like clumpy charge regions, especially during the plume growth period. This idea was first proposed by Behnke et al. (2013), based on observations of Redoubt volcano, to explain temporal changes in VHF source distributions. This complex structure has also been proposed as a possible mechanism in volcanic lightning experiments (Cimarelli et al., 2014). Because the charges are highly disorganized in space, negative and positive lightning may occur at comparable frequencies. On the other hand, negative lightning dominates in thunderclouds (Rakov and Uman, 2003). Based on static vertical electric field measurements at Sakurajima, Lane and Gilbert (1992) proposed bipolar charge structures in the plume, comprising a positive charge in an upper gas region above the plume and a negative charge in the plume itself. Miura et al. (2002) suggested a tripolar structure, consisting of a positive charge in an upper gas region, a negative charge in fine plume ash, and positive charge pockets in coarse ash at the base of the plume. However, the previously inferred ordered charge structures were determined by averaged observations made after the explosion, when the plume had already reached its buoyant phase; ejected particles were already segregated by size, and gas had partly decoupled from the larger particles. Therefore, the charge structure at the inception of each explosion was not investigated. Based on the volcanic lightning observations, we suggest that the initial charge structure is highly disorganized and complex during the first phase of plume growth, due to turbulent jetting. During this phase, most of the discharges are observed at 0–350 m above the vent, where the maximum velocities of ballistic projectiles can reach up to 120 m/s (Cimarelli et al., in press).

The relatively large proportion of +CG in volcanic lightning may not be explained solely by complex charge distribution in the plume. Although charge structure is considered to be progressively organized after an eruption onset, the occurrences of +CG and −CG show a similar time dependence (Fig. 7b). This result indicates either that the gross charge structures estimated in previous studies (Lane and Gilbert, 1992; Miura et al., 2002) are not common during lightning occurrences, and/or that other factors contribute to the polarity of volcanic lightning. As an example of the latter, winter lightning in Hokuriku, Japan, is similar to volcanic lightning at Sakurajima, in that the proportion of +CG is very high (Takeuti et al., 1978), yet Brook et al. (1982) found strong correlations between the fraction of positive ground strokes and vertical wind shear in the cloud layer. It has also been suggested that the proportion of +CG is high in severe thunderstorms, possibly due to the high content of liquid water and the broad size of the updraft (Carey and Buffalo, 2007). However, these relationships could not be investigated in this study. Future experiments will examine possible correlations between discharge polarity, wind shear, and plume dynamics.

Despite its small scale, volcanic lightning seems to generate a high number of return strokes (as estimated from Type A impulses) per lightning event, which is comparable to the return-stroke multiplicity of thunderstorm lightning. Although studies of thunderstorm lightning clearly demonstrate the relatively small number of return strokes in +CG (Rakov and Huffines, 2003; Saba et al., 2007), our observations differ in the sense that volcanic lightning at Sakurajima has, relatively speaking, many +CG events and many return strokes in a lightning event. This return-stroke multiplicity may also be related to the complex charge structure. Because the charges are highly disorganized in space, stepped leaders may not carry charges effectively from a volcanic plume, consequently resulting in multiple return strokes.

The physical properties and mechanisms of Type B discharges, which are interpreted as IC, remain unclear. Typical waveforms of meteorological intra-cloud lightning are similar to our observations (Kitagawa and Brook, 1960; Zhu et al., 2014). We speculate that Type B discharges may be similar to those of thunderstorm lightning (Kitagawa and Brook, 1960; Ogawa and Brook, 1964).

The scope of this paper is limited to a comparison between the physical properties of volcanic and thunderstorm lightning. Although the generation mechanism of volcanic lightning is beyond this scope, we briefly make one remark on this topic. Fig. 7 shows that CG occurs mainly at 5–20 s after eruption onset. From similar results, Aizawa et al. (2010) suggested that a preparatory process, such as charge generation and/or separation, is required for CG lightning to occur and for corresponding MT pulses to be generated and recorded. Two possible mechanisms were considered for the generation of the necessary electric field: continuous collision between particles in the plume, and gravitational charge separation. On the other hand, we occasionally observed numerous small IC flashes occurring just after eruption onset in NS videos (Supplementary material). This suggests that electrification may also occur in the crater, at the vent, and possibly within the conduit. Explosions at Showa crater are caused by the fragmentation of semi-solidified magma plugs stagnating in the shallow conduit of the volcano (Yokoo et al., 2013). Thus, we do not exclude magmatic fragmentation (e.g., Mather and Harrison, 2006; James et al., 2008) as a possible electrification mechanism. In addition, seismic records show that eruptions at Sakurajima are preceded by precursory 'explosion earthquakes' that occur ∼1 s before the eruption (Tameguri et al., 2002). Although the nature of the 'explosion earthquakes' has yet to be clarified, the events occur at ∼1 km below sea level, which is the estimated depth of an aquifer beneath the volcano (Aizawa et al., 2011). Therefore, both magma–water interactions and the boiling of water, along with subsequent electrification, might occur at depth, at ∼1 s before an eruption. The previously suggested mechanisms (magma fragmentation, boiling of water, magma–water interaction, and particle–particle collisions; e.g., Buttner et al., 2000; James et al., 2000; Mather and Harrison, 2006; James et al., 2008) may jointly contribute to the electrification.

5. Conclusions

Volcanic lightning, and more broadly the electrical properties of volcanic plumes, are attracting increasing scientific interest, both in volcanology and other fields of inquiry, on account of the implications of such lightning for the origin and early evolution of life on Earth, as well as the impacts of volcanic lightning on the atmosphere of Earth and other planets (Navarro-Gonzalez et al., 1998; Mather et al., 2004b; James et al., 2008). However, due to the limited number of studies dedicated to volcanic lightning, the physical mechanisms and properties of such lightning have yet to be thoroughly explored. In this study, we conducted joint high-sampling-rate MT and high-speed video observations to investigate the physical properties of vent discharges and near-vent volcanic lightning at Sakurajima, Japan. Employing high-sensitivity and high-sampling-rate MT observations, we detected EM signals from volcanic lightning close to the crater. The detection efficiency depends on the signal-to-noise ratio between EM radiation from lightning and military VLF noise; 90.1% of optical emissions visible in normal-speed (30 fps) videos generate MT signals at approximately 2.2 and 3.5 km from Showa crater. By careful inspection of all MT waveforms that synchronized with the visible flashes, we identified two categories of discharges. The first consists of single or multiple impulses (Type A). Very luminous flashes in the videos always correspond to Type A discharges. The second resembles EM variations with multiple peaks whose inter-pulse repose times are not well-characterized (Type B). By comparing MT data with video recordings, Type B discharges are interpreted as IC lightning. According to our observations, CG lightning always corresponds to

Type A discharges, but we do not deny the possibility that some IC events exhibit Type A discharges. The estimated physical parameters are consistent with the picture that volcanic lightning is a miniature-scale equivalent of thunderstorm lightning in many respects. The overall duration, length, inter-stroke interval, peak current, and charge transfer all have values 1–2 orders of magnitude smaller than those of thunderstorm lightning. This suggests a scaling relation between volcanic and thunderstorm lightning parameters that is independent of the type of charged particles. On the other hand, polarity differ from thunderstorm lightning. We speculate that the difference is due to the complexity of charge structures within eruption plumes. Previous studies of volcanic lightning (e.g., reviews by Mather and Harrison, 2006; McNutt and Williams, 2010, and references therein) sometimes implicitly assumed that volcanic lightning has a similar physical mechanism to thunderstorm lightning, but this has not yet been fully confirmed. Our observations presented here thus provide basic information about the similarities of and differences between volcanic and thunderstorm lightning.

Joint MT and high-speed video observations provide constraints on the nature of volcanic lightning. Similar observations at other active volcanoes are encouraged to further constrain the physical properties of volcanic lightning. In addition, observations at higher sampling rates (over 100 kHz) would provide more detailed information, such as the evolution of lightning channel, precise stroke waveforms, and better characterization of IC discharges. Nevertheless, both kinds of observations present some limitations. Despite their detailed precision in picturing the electrical discharges, HS video observations cannot capture all lightning, being limited to visible flashes around and within the plume. MT data also have limited utility for accurately locating events, as vertical lightning must be assumed. Although time-of-arrival techniques are feasible in MT, they require observation sites located far from the crater, which would greatly reduce sensitivity. Further collocation with VHF or LF/MF lightning locating systems would thus be a useful innovation to be investigated in future work.

Acknowledgements

We are greatly indebted to land owners for the prolonged hosting of MT stations. We thank the Earthquake Research Institute of the University of Tokyo for the loan of two sets of MT apparatuses (KYODO-RIYO CODE 2013-F-07), and the staff of Sakurajima Volcano Observatory, Kyoto University, Japan, for valuable assistance during fieldwork. Bettina Scheu and Sebastian Mueller are acknowledged for their contribution to HS video observations. Constructive suggestions and comments from two anonymous reviewers and from the editor, Tamsin Mather, greatly improved the manuscript. Plume height data were obtained from the Japan Meteorological Agency (JMA). This work was supported by MEXT KAKENHI Grant Number 23740332. CC and MA were supported by the AXA Research Fund "Risk from volcanic ash in the Earth System". DBD acknowledges the support of ERC Advanced Grant No. 247076: (EVOKES – Explosive Volcanism in the Earth System).

Appendix A. Supplementary material

Supplementary material related to this article can be found online at http://dx.doi.org/10.1016/j.epsl.2016.03.024.

References

Aizawa, K., Kanda, W., Ogawa, Y., Iguchi, M., Yokoo, A., Yakiwara, H., Sugano, T., 2011. Temporal changes in electrical resistivity at Sakurajima volcano from continuous magnetotelluric observations. J. Volcanol. Geotherm. Res. 199, 165–175. http://dx.doi.org/10.1016/j.jvolgeores.2010.11.003.

Aizawa, K., Yokoo, A., Kanda, W., Ogawa, Y., Iguchi, M., 2010. Magnetotelluric pulses generated by volcanic lightning at Sakurajima volcano, Japan. Geophys. Res. Lett. 37. http://dx.doi.org/10.1029/2010gl044208.

Anderson, R., Bjornsso, S., Blanchar, D.C., Gathman, S., Hughes, J., Jonasson, S., Moore, C.B., Survilas, H.J., Vonnegut, B., 1965. Electricity in volcanic clouds – investigations show that lightning can result from charge-separation processes in a volcanic crater. Science 148, 1179–1189.

Arason, P., Bennett, A.J., Burgin, L.E., 2011. Charge mechanism of volcanic lightning revealed during the 2010 eruption of Eyjafjallajokull. J. Geophys. Res., Solid Earth 116. http://dx.doi.org/10.1029/2011jb008651.

Ballarotti, M.G., Medeiros, C., Saba, M.M.F., Schulz, W., Pinto Jr., O., 2012. Frequency distributions of some parameters of negative downward lightning flashes based on accurate-stroke-count studies. J. Geophys. Res., Atmos. 117. http://dx.doi.org/10.1029/2011jd017135.

Ballarotti, M.G., Saba, M.M.F., Pinto, O., 2005. High-speed camera observations of negative ground flashes on a millisecond-scale. Geophys. Res. Lett. 32. http://dx.doi.org/10.1029/2005gl023889.

Behnke, S.A., Bruning, E.C., 2015. Changes to the turbulent kinematics of a volcanic plume inferred from lightning data. Geophys. Res. Lett. 42, 4232–4239. http://dx.doi.org/10.1002/2015gl064199.

Behnke, S.A., McNutt, S.R., 2014. Using lightning observations as a volcanic eruption monitoring tool. Bull. Volcanol. 76. http://dx.doi.org/10.1007/s00445-014-0847-1.

Behnke, S.A., Thomas, R.J., Edens, H.E., Krehbiel, P.R., Rison, W., 2014. The 2010 eruption of Eyjafjallajökull: lightning and plume charge structure. J. Geophys. Res., Atmos. 119. http://dx.doi.org/10.1002/2013JD020781.

Behnke, S.A., Thomas, R.J., McNutt, S.R., Schneider, D.J., Krehbiel, P.R., Rison, W., Edens, H.E., 2013. Observations of volcanic lightning during the 2009 eruption of Redoubt Volcano. J. Volcanol. Geotherm. Res. 259, 214–234. http://dx.doi.org/10.1016/j.jvolgeores.2011.12.010.

Bennett, A.J., Odams, P., Edwards, D., Arason, P., 2010. Monitoring of lightning from the April–May 2010 Eyjafjallajokull volcanic eruption using a very low frequency lightning location network. Environ. Res. Lett. 5. http://dx.doi.org/10.1088/1748-9326/5/4/044013.

Berger, K., Anderson, R.B., Kroniger, H., 1975. Parameters of lightning flashes. Electra 41, 23–37.

Betz, H.D., Schmidt, K., Laroche, P., Blanchet, P., Oettinger, W.P., Defer, E., Dziewit, Z., Konarski, J., 2009. LINET—an international lightning detection network in Europe. Atmos. Res. 91, 564–573. http://dx.doi.org/10.1016/j.atmosres.2008.06.012.

Bitzer, P.M., Christian, H.J., Stewart, M., Burchfield, J., Podgorny, S., Corredor, D., Hall, J., Kuznetsov, E., Franklin, V., 2013. Characterization and applications of VLF/LF source locations from lightning using the Huntsville Alabama Marx Meter Array. J. Geophys. Res., Atmos. 118, 3120–3138. http://dx.doi.org/10.1002/jgrd.50271.

Brook, M., Moore, C.B., Sigurgei, T., 1974. Lightning in volcanic clouds. J. Geophys. Res. 79, 472–475. http://dx.doi.org/10.1029/JC079i003p00472.

Brook, M., Nakano, M., Krehbiel, P., Takeuti, T., 1982. The electrical structure of the Hokuriku winter thunderstorms. J. Geophys. Res., Oceans Atmos. 87, 1207–1215. http://dx.doi.org/10.1029/JC087iC02p01207.

Buttner, R., Zimanowski, B., Roder, H., 2000. Short-time electrical effects during volcanic eruption: experiments and field measurements. J. Geophys. Res., Solid Earth 105, 2819–2827. http://dx.doi.org/10.1029/1999jb900370.

Carey, L.D., Buffalo, K.M., 2007. Environmental control of cloud-to-ground lightning polarity in severe storms. Mon. Weather Rev. 135, 1327–1353. http://dx.doi.org/10.1175/mwr3361.1.

Carey, S.N., Sigurdsson, H., 1982. Influence of particle aggregation on deposition of distal tephra from the May 18, 1980, eruption of Mount St-Helens volcano. J. Geophys. Res. 87, 7061–7072. http://dx.doi.org/10.1029/JB087iB08p07061.

Chave, A.D., Jones, A.G., 2012. The Magnetotelluric Method. Cambridge Univ. Press, New York, 552 pp.

Cimarelli, C., Alatorre-Ibarguengoitia, M.A., Aizawa, K., Yokoo, A., Iguchi, M., Dingwell, D.B., in press. Multiparametric observation of volcanic lightning at Sakurajima volcano, Japan. Geophys. Res. Lett. http://dx.doi.org/10.1002/2015GL067445.

Cimarelli, C., Alatorre-Ibarguengoitia, M.A., Kueppers, U., Scheu, B., Dingwell, D.B., 2014. Experimental generation of volcanic lightning. Geology 42, 79–82. http://dx.doi.org/10.1130/g34802.1.

Fisher, R.J., Schnetzer, G.H., Thottappillil, R., Rakov, V.A., Uman, M.A., Goldberg, J.D., 1993. Parameters of triggered-lightning flashes in Florida and Alabama. J. Geophys. Res., Atmos. 98, 22887–22902. http://dx.doi.org/10.1029/93jd02293.

James, M.R., Lane, S.J., Gilbert, J.S., 2000. Volcanic plume electrification: experimental investigation of a fracture-charging mechanism. J. Geophys. Res., Solid Earth 105, 16641–16649. http://dx.doi.org/10.1029/2000jb900068.

James, M.R., Wilson, L., Lane, S.J., Gilbert, J.S., Mather, T.A., Harrison, R.G., Martin, R.S., 2008. Electrical charging of volcanic plumes. Space Sci. Rev. 137, 399–418. http://dx.doi.org/10.1007/s11214-008-9362-z.

Kitagawa, N., 2005. Substantial mechanisms of step-voltage effects. In: Pontikis, C. (Ed.), Recent Progress in Lightning Physics. Res. Signpost, Kerala, India, pp. 23–32.

Kitagawa, N., Brook, M., 1960. A comparison of intracloud and cloud-to-ground lightning discharges. J. Geophys. Res. 65, 1189–1201. http://dx.doi.org/10.1029/JZ065i004p01189.

Lane, S.J., Gilbert, J.S., 1992. Electric-potential gradient changes during explosive activity at Sakurajima volcano, Japan. Bull. Volcanol. 54, 590–594. http://dx.doi.org/10.1007/bf00569942.

Mather, T.A., Allen, A.G., Davison, B.M., Pyle, D.M., Oppenheimer, C., McGonigle, A.J.S., 2004a. Nitric acid from volcanoes. Earth Planet. Sci. Lett. 218, 17–30. http://dx.doi.org/10.1016/s0012-821x(03)00640-x.

Mather, T.A., Harrison, R.G., 2006. Electrification of volcanic plumes. Surv. Geophys. 27, 387–432. http://dx.doi.org/10.1007/s10712-006-9007-2.

Mather, T.A., Pyle, D.M., Allen, A.G., 2004b. Volcanic source for fixed nitrogen in the early Earth's atmosphere. Geology 32, 905–908. http://dx.doi.org/10.1130/g20679.1.

Mazur, V., Krehbiel, P.R., Shao, X.M., 1995. Correlated high-speed video and radio interferometric observations of a cloud-to-ground lightning flash. J. Geophys. Res., Atmos. 100, 25731–25753. http://dx.doi.org/10.1029/95jd02364.

McNutt, S.R., Davis, C.M., 2000. Lightning associated with the 1992 eruptions of Crater Peak, Mount Spurr Volcano, Alaska. J. Volcanol. Geotherm. Res. 102, 45–65.

McNutt, S.R., Williams, E.R., 2010. Volcanic lightning: global observations and constraints on source mechanisms. Bull. Volcanol. 72, 1153–1167. http://dx.doi.org/10.1007/s00445-010-0393-4.

Miura, T., Koyaguchi, T., Tanaka, Y., 2002. Measurements of electric charge distribution in volcanic plumes at Sakurajima Volcano, Japan. Bull. Volcanol. 64, 75–93. http://dx.doi.org/10.1007/s00445-001-0182-1.

Navarro-Gonzalez, R., Molina, M.J., Molina, L.T., 1998. Nitrogen fixation by volcanic lightning in the early Earth. Geophys. Res. Lett. 25, 3123–3126. http://dx.doi.org/10.1029/98gl02423.

Ogawa, T., Brook, M., 1964. Mechanism of intracloud lightning discharge. J. Geophys. Res. 69, 5141. http://dx.doi.org/10.1029/JZ069i024p05141.

Rakov, A.V., Uman, M.A., 2003. Lightning – Physics and Effects. Cambridge Univ. Press, New York. 687 pp.

Rakov, V.A., Huffines, G.R., 2003. Return-stroke multiplicity of negative cloud-to-ground lightning flashes. J. Appl. Meteorol. 42, 1455–1462. http://dx.doi.org/10.1175/1520-0450(2003)042<1455:rmoncl>2.0.co;2.

Saba, M.M.F., Ballarotti, M.G., Campos, L.Z.S., Osmar, P., 2007. High-speed video observations of positive lightning, paper presented. In: IX International Symposium on Lightning Protection. Institute of Electrotechnology and Energy, Foz do Iguaçu, Brazil.

Shao, X.M., Stanley, M., Regan, A., Harlin, J., Pongratz, M., Stock, M., 2006. Total lightning observations with the new and improved Los Alamos Sferic Array (LASA). J. Atmos. Ocean. Technol. 23, 1273–1288. http://dx.doi.org/10.1175/jtech1908.1.

Simpson, F., Bahr, K., 2005. Practical Magnetotellurics. Cambridge Univ. Press, Cambridge. 254 pp.

Takeuti, T., Nakano, M., Brook, M., Raymond, D.J., Krehbiel, P., 1978. Anomalous winter thunderstorms of Hokuriku coast. J. Geophys. Res., Oceans Atmos. 83, 2385–2394. http://dx.doi.org/10.1029/JC083iC05p02385.

Tameguri, T., Iguchi, M., Ishihara, K., 2002. Mechanism of explosive eruptions from moment tensor analyses of explosion earthquakes at Sakurajima volcano, Japan. Bull. Volcanol. Soc. Jpn. 47, 197–215.

Thomas, R.J., Krehbiel, P.R., Rison, W., Edens, H.E., Aulich, G.D., Winn, W.P., McNutt, S.R., Tytgat, G., Clark, E., 2007. Electrical activity during the 2006 Mount St. Augustine volcanic eruptions. Science 315, 1097. http://dx.doi.org/10.1126/science.1136091.

Thomas, R.J., McNutt, S.R., Krehbiel, P.R., William, R., Aulich, G., Edens, H.E., Tytgat, G., Clark, E., 2012. Lightning and electrical activity during the 2006 eruption of Augustine volcano. In: Power, J.A., Coombs, M.L., Freymueller, J.T. (Eds.), U.S. Geological Survey Professional Paper, vol. 1769, pp. 579–608.

Uman, M.A., Lin, Y.T., Krider, E.P., 1980. Errors in magnetic direction finding due to nonvertical lightning channels. Radio Sci. 15, 35–39. http://dx.doi.org/10.1029/RS015i001p00035.

Visacro, S., Soares, A., Schroeder, M.A.O., Cherchiglia, L.C.L., de Sousa, V.J., 2004. Statistical analysis of lightning current parameters: measurements at Morro do Cachimbo Station. J. Geophys. Res., Atmos. 109. http://dx.doi.org/10.1029/2003jd003662.

Yokoo, A., Iguchi, M., Tameguri, T., Yamamoto, K., 2013. Processes prior to outburst of vulcanian eruption at Showa crater of Sakurajima volcano. Bull. Volcanol. Soc. Jpn. 58, 163–181.

Yokoo, A., Tameguri, T., Iguchi, M., 2009. Swelling of a lava plug associated with a Vulcanian eruption at Sakurajima Volcano, Japan, as revealed by infrasound record: case study of the eruption on January 2, 2007. Bull. Volcanol. 71, 619–630. http://dx.doi.org/10.1007/s00445-008-0247-5.

Zhu, B.Y., Zhou, H.L., Thottappillil, R., Rakov, V.A., 2014. Simultaneous observations of electric field changes, wideband magnetic field pulses, and VHF emissions associated with K processes in lightning discharges. J. Geophys. Res., Atmos. 119, 2699–2710. http://dx.doi.org/10.1002/2013jd021006.